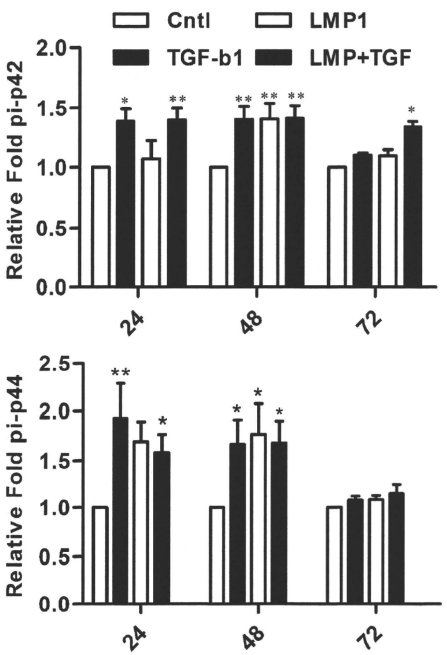

Figure S2. LMP1 and TGF-β1 induce sustained ERK signaling in A549. Densitometric analysis of 6 separate western blots of which figure 6B is representative.
118x165mm (600 x 600 DPI)

Figure S3

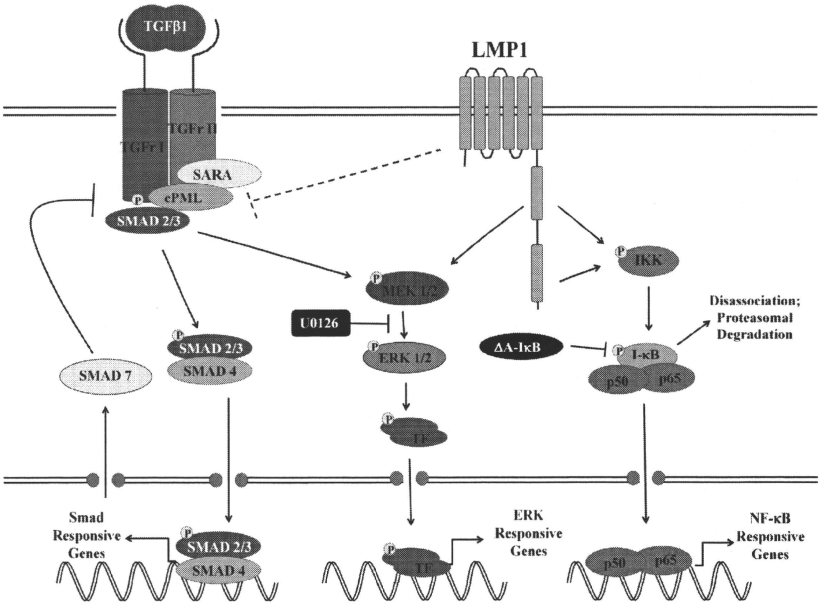
TGFβ1
LMP1
TGFr II
TGFr I
SARA
cPML
SMAD 2/3
MEK 1/2
U0126
ERK 1/2
IKK
ΔA-IκB
I-κB
p50
p65
Disassociation;
Proteasomal
Degradation
SMAD 7
SMAD 2/3
SMAD 4
TF
Smad
Responsive
Genes
ERK
Responsive
Genes
NF-κB
Responsive
Genes

DOI:10.1158/1078-0432.CCR-10-0659

Imaging, Diagnosis, Prognosis

Clinical Cancer Research

Neurotensin Receptor 1 Determines the Outcome of Non–Small Cell Lung Cancer

Marco Alifano[1], Frédérique Souazé[3], Sandra Dupouy[2], Sophie Camilleri-Broët[4], Mohamad Younes[2], Sadi-Menad Ahmed-Zaïd[2], Takashi Takahashi[5], Alessandra Cancellieri[6], Stefania Damiani[7], Maurizio Boaron[7], Philippe Broët[4], Lance D. Miller[8], Christian Gespach[2], Jean François Regnard[1], and Patricia Forgez[2]

Abstract

Purpose: This study aimed to investigate the role of the neurotensin/neurotensin receptor I (NTSR1) complex in non–small cell lung cancer (NSCLC) progression.

Experimental Design: The expression of neurotensin and NTSR1 was studied by transcriptome analysis and immunohistochemistry in two series of 74 and 139 consecutive patients with pathologic stage I NSCLC adenocarcinoma. The findings were correlated with clinic-pathologic features. Experimental tumors were generated from the malignant human lung carcinoma cell line A459, and a subclone of LNM35, LNM-R. The role of the neurotensin signaling system on tumor growth and metastasis was investigated by small hairpin RNA–mediated silencing of NTSR1 and neurotensin.

Results: Transcriptome analysis carried out in a series of 74 patients showed that the positive regulation of *NTSR1* put it within the top 50 genes related with relapse-free survival. Immunohistochemistry revealed neurotensin- and NTSR1-positive staining in 60.4% and 59.7% of lung adenocarcinomas, respectively. At univariate analysis, NTSR1 expression was strongly associated with worse 5-year overall survival rate ($P = 0.0081$) and relapse-free survival ($P = 0.0024$). Multivariate analysis showed that patients over 65 years of age ($P = 0.0018$) and NTSR1 expression ($P = 0.0034$) were independent negative prognostic factors. Experimental tumor xenografts generated by neurotensin- and NTSR1-silenced human lung cancer cells revealed that neurotensin enhanced primary tumor growth and production of massive nodal metastasis via autocrine and paracrine regulation loops.

Conclusion: NTSR1 expression was identified as a potential new prognostic biomarker for surgically resected stage I lung adenocarcinomas, as NTSR1 activation was shown to participate in lung cancer progression. *Clin Cancer Res; 16(17); 4401–10. ©2010 AACR.*

Lung cancer is the leading cause of cancer-related deaths in the United States and remains the most common malignancy in the world (1–3). Two main histologic categories are recognized: small cell lung cancer and non–small cell lung cancer (NSCLC). NSCLC is usually further divided into three main histologic types: large cell lung carcinoma, squamous cell carcinoma, and adenocarcinoma. This last represents nowadays the most frequent histologic type in western countries. NSCLC is believed to arise from a multistep process, with each step associated with genetic and epigenetic alterations, and correlated with tumor aggressiveness. The factors used to define the stage of the disease, to choose the optimal management, and to predict outcome are the size of the primary tumor, the invasion of locoregional nodes, and the presence of distant metastases (4). Nevertheless, a vast disparity in patient outcome is seen within the same stage. Globally, patients with operable lung cancers (stage I-IIIa) have an overall 5-year survival rate of around 40%. The survival rate among those with stage I disease is only 60% to 70%; in a quarter of these patients relapse is local, whereas for the others the disease shows metastatic spread (4–6). The current challenge today is to identify factors that would predict tumor relapse despite curative treatment. In a series of stage IB lung adenocarcinomas, we carried out a tandem DNA copy number and gene expression profile using high-resolution microarrays to establish a robust predictor of clinical outcome

Authors' Affiliations: [1]Service de chirurgie thoracique, Hôtel-Dieu, and [2]INSERM-UPMC U 938, Paris, France; [3]EA-4273 Biometadys, Faculté de Médecine, Nantes, France; [4]JE2492, Université Paris-Sud, Villejuif, France; [5]Center for Neurological Diseases and Cancer, Nagoya, Japan; [6]Pathology Department and [7]Thoracic Surgery Department, Maggiore-Bellaria Hospital, Bologna, Italy; and [8]Wake Forest University School of Medicine, Medical Center, North Carolina

Note: Supplementary data for this article are available at Clinical Cancer Research Online (http://clincancerres.aacrjournals.org/).

M. Alifano, F. Souazé, and S. Dupouy contributed equally to this work.

Corresponding Author: Patricia Forgez, INSERM, Pav Raoul Kourilsky, Hopital Saint-Antoine, 184 rue du Fbg Saint-Antoine, Paris, 75012 France. Phone: 33-1-49-28-46-74; Fax: 33-1-49-28-46-38; E-mail: patricia.forgez@inserm.fr.

doi: 10.1158/1078-0432.CCR-10-0659

DOI:10.1158/1078-0432.CCR-10-0659

Translational Relevance

Non-small cell lung cancer is a heterogeneous condition with significant variability in prognosis and in the individual response to treatments. Therefore, identification of patients with high risk of relapse after surgery will enable tailored management in terms of adjuvant treatments and stricter follow-up. We report that the neurotensin/neurotensin receptor 1 (NTSR1) complex is specifically expressed in lung adenocarcinoma. NTSR1 expression was identified as an independent predictive marker of unfavorable outcome in stage I lung adenocarcinoma treated by surgery alone. Experimental data suggest that the neurotensin/NTSR1 complex is an enhancer of lung tumor progression. The neurotensin system is therefore suitable for the development of new therapeutic targets, new applications of already available treatments, and the development of a new diagnostic biomarker ensuing better predictive parameters.

at the early stages of NSCLC (7). Among the first 50 genes upregulated and associated with disease-free survival was the neurotensin receptor 1 (*NTSR1*).

Neurotensin and its cognate receptor (NTSR1) are neuropeptide-receptor complexes frequently deregulated during the neoplastic process. Neurotensin is a 13-amino-acid peptide previously recognized for its distribution along the gastrointestinal tract (8). Typical physiologic functions associated with neurotensin include the stimulation of pancreatic and biliary secretions, inhibition of small bowel and gastric motility, and facilitation of fatty acids translocation (9, 10). The peripheral functions of neurotensin are mediated through its interaction with NTSR1, a high affinity receptor coupled to a Gq/G11 protein. When neurotensin binds to NTSR1, phosphatidyl inositols are hydrolyzed leading to Ca2+ mobilization and PKC activation.

NTSR1 activation leads to cell proliferation, survival, mobility, and invasiveness in specific cancer cell types via signal transduction through PKC, extracellular signal-regulated kinase 1 and 2, RhoGTPases, NF-κB, or focal adhesion kinase activation. (11–13). The disruption of the neurotensinergic pathway through a specific antagonist, in experimental tumors from colon, breast, and small cell lung cancer cells, caused a strong reduction in tumor growth (14–16). We had previously shown the presence of a chronic self-activation loop between neurotensin and NTSR1, as one mechanism responsible for the constitutive activation of the mitogen-activated protein kinase mitogenic signaling pathways along with sustained target gene activation (17–20). More recently, NTSR1 expression level was associated with poor prognosis in patients with ductal breast cancer, and similar results have been found in head and neck squamous cell carcinomas (21, 22).

In this study, we examined the expression of both neurotensin and NTSR1 in two series of consecutive patients undergoing pulmonary lobectomy and nodal dissection for pathologic stage I lung adenocarcinoma by transcriptome analysis and immunohistochemistry, respectively. The expression of NTSR1 was clearly shown to negatively affect the outcome. Experimental tumors were also developed to study the role of the neurotensin system on tumor growth. With this model, we show the aggravating role of the neurotensinergic system in tumor progression.

Materials and Methods

Study from a genome-wide gene expression

We report the results obtained for NTSR1 from a previous large-scale gene expression analysis carried out on 74 homogeneous cases of stage pT_2N_0 lung adenocarcinomas/large cell carcinomas treated by surgery (7). In this study RNA samples were hybridized to the Human U133 Plus 2.0 oligonucleotide arrays (Affymetrix), and 37,771 probes met the quality control criteria and were considered for the analysis (GEO Series accession number GSE10445). We selected transcripts having a high likelihood of being associated with relapse-free survival (RFS) by considering the false discovery rate error as described in Broet et al. (7).

Patients and tissue specimens for neurotensin and NTSR1 immunohistochemistry

Expression of NTSR1 and neurotensin was done in a multicenter study. The clinical files of 139 patients (Table 1) treated by lobectomy and full nodal dissection for pathologic stage I (pT_1N_0, $n = 51$; pT_2N_0, $n = 88$) primary lung adenocarcinomas were retrospectively reviewed. They were operated on in three teaching hospitals in Paris, France and Bologna, Italy between January 2001 and March 2003. All patients had macroscopically and microscopically complete resections. None of the patients had preoperative or postoperative chemotherapy or radiotherapy. For all cases histologic slides of primary tumors were obtained by paraffin wax embedded tissues. Standard H&E staining was used to ensure the tumoral character of the specimen, and adjacent sections were obtained for immunohistochemistry. For 23 of 71 patients operated on at the Hôtel-Dieu Hospital, frozen samples of resected tumors were used to detect RNA for neurotensin and NTSR1, after verification of the tumoral character of the samples by frozen sections. As normal tissue, we assessed the lung parenchyma of 26 patients with idiopathic pneumothorax treated by apical resection.

Ethics

The study was carried out according to the Declaration of Helsinki principles and in agreement with the French and Italian laws on biomedical research. The following studies were conducted on tissues obtained from surgical specimens between 2001 and 2003. The experiments reported here were carried out under the current ethical

DOI:10.1158/1078-0432.CCR-10-0659

regulations as defined by the Huriet-Sérusclat Act of December 20, 1988. Under this act, institutional review board approval was not required. Accordingly, patients or next of kin (in case of deceased patients) were specifically asked for verbal informed consent only.

Statistical analysis

Overall survival rates were estimated using the Kaplan-Meier method, and survival curves were compared using the Log-rank test. RFS time was calculated from the date of the patients' surgery until disease-related death, disease recurrence (either local or distant), or last follow-up examination. All available variables potentially influencing survival, namely, age, sex, smoking habit (current and former versus never smoker), presence of vascular or lymphatic or vascular emboli, pT category, and NTSR1 expression, were considered for a multivariate analysis using the Cox proportional hazards model.

For the transcriptome analysis, the prognostic impact of *NTSR1* gene expression changes on RFS was evaluated by calculating the score test statistic derived from the semi-parametric Cox proportional hazards model. The analyses were done with the SPlus software package.

Immunohistochemistry

Immunostaining of neurotensin and NTSR1 was carried out on 4-μm-thick deparaffinized sections, using the avidin-biotin-peroxidase complex method. Slides were incubated with 10% normal rabbit serum at room temperature for 30 minutes. Neurotensin immunoreactivity was conducted using rabbit antibody directed against neurotensin (1:500; NA1230, Biomol GmbH) for 2 hours. NTSR1 immunoreactivity was detected using a goat polyclonal antibody directed against the human carboxy terminus of the receptor (1:100; C-20, Santa Cruz Biotechnology). All slides were rinsed three times with TBS; sections were incubated with biotinylated secondary antibody (1:200; Vector laboratories, Inc). The antigen-antibody complex was revealed with avidin-biotin-peroxidase complex, according to the manufacturer's instructions for the Vectastain ABC Kit (Vector laboratories, Inc.). Staining was done with diamino-benzidine tetrahydrochlorid. All slides were counterstained with hematoxylin. All specimens were scored by an anatomopathologist (SCB).

Culture procedures

The human lung adenocarcinoma cell lines LNM35 and A459 were grown in RPMI-1640 medium (Invitrogen

Table 1. Clinical characteristics of the multicenter series of patients whose tumors were studied by immunohistochemistry for neurotensin and NTSR1 expression

Lung adenocarcinomas, *n* = 139	
Age (years)	64.0 ± 10.7
Women	34/139 (24.5%)
Tobacco history	
Current smoker	71
Former smoker (stop >2 months)	49
Never smoker	19
pT_1 disease	51/139 (36.7%)
pT_2 disease	88/139 (63.3%)
Tumor size (cm), mean ± SD	3.1 ± 1.94
N_0	139/139
Intratumoral or peritumoral neoplastic vascular emboli	34/139 (24.5%)
Intratumoral or peritumoral neoplastic lymphatic emboli	21/139 (15.1%)
NTSR1-positive tumors, *n* (% of patients)	83/139 (59.7%)
Neurotensin -positive tumors, *n* (% of patients)	84/139 (60.4%)
NTSR1- and neurotensin-positive tumors, *n* (% of patients)	54/139 (38.8%)
Lost at follow-up	1/139 (0.7%)
Follow-up in months, mean ± SD	44.2 ± 20.9
Deaths during follow-up, *n* (% of patients)	49/139 (31%)
Perioperative therapies	
Radiotherapy	0/139
Chemotherapy	0/139
Idiopathic pneumothorax, *n* = 26	
NTSR1-positive lung parenchyma	0/26
Neurotensin-positive lung parenchyma	0/26
NTSR1- and neurotensin-positive lung parenchyma	0/26

DOI:10.1158/1078-0432.CCR-10-0659

SARL) supplemented with 10% FCS and 2 mmol/L glutamine (23). The LNM35 cell line was subcloned by limiting dilution; clones containing exclusively rounded cells were named LNM-R.

NTSR1 and neurotensin siRNA construction and transfection. Small hairpin RNAs for human NTSR1 (AAGAAGTTCATCAGCGCCATC) and neurotensin (5′-GCAATGTTGACAATATACC-3′) were prepared using psilencer 3.1-H1 according to the manufacturer's instruction. LNM-R and A549 cells were transfected using the Lipofectamine reagent (20).

Experimental tumors

Xenografts were initiated in nude mice by s.c. injection of 10^6 cells of LNM-R and derivative cell clones, or 10^7 cells of A549 and A549 NTSR1-silenced clones. For tumors generated from a cell mixture, 10^6 cells from each clone were plated together 72 hours prior to injection. Four to six series were done; each series included 5 to 8 mice. The tumor volume was calculated with the ellipsoid formula.

RNA extraction and reverse transcriptase-PCR. The protocols for total RNA extraction, reverse-transcription reaction, and PCR are documented in detail in Souazé et al. (24). Reverse-transcription reaction was done on 2 μg of total RNA using a specific NTSR1 primer (5′-GCTGACGTAGAAGAG-3′) or 50 pmol of oligo dT and oligo dN. The PCR amplification was done on a 1:5 v/v of the reverse-transcription reaction using 25 pmol of each primer 5′-CGTGGAGCTGTACAACTTCA-3′ and 5′-CAGCCAGCAGACCACAAAGG-3′ for NTSR1, and 5′-CAGCTCCTGGAGTCTGTGCT-3′ and 5′-GTTGAAAAGCCCTGCTGTGACAGA-3′ for neurotensin, 5′-TCAAATGAGATTGTGGAAAA-3 and AS 5-AGATCATCTCTGCCTGAGTAT-3′ for cyclooxygenase-2, 5′-CGGAGTCAACGGATTTGGTCG-3′ and 5′-TTCACCACCATGGAGAAGGCT-3′ for GAPDH, and 1 unit of Taq polymerase.

Neurotensin RIA

One million cells were grown in 60 mm^2 Petri dishes. After 24 hours media were removed and serum-free media were added to the cells for 24, 48, or 72 hours. Media were collected; centrifuged 5 minutes at 2,000 *g*, and 5,000 UIK/mL of trasylol was added to the supernatant. RIA was done on 1 mL of lyophilized media according the procedure developed in Scarceriaux et al. (25).

Results

Genome-wide gene expression study in a population of patients with lung adenocarcinoma/large cell carcinomas

In an attempt to identify a clinical outcome predictor for patients with NSCLC, patterns of genomic alteration and gene expression profiles were analyzed and integrated concerning 74 homogeneous cases of stage Ib pT_2N_0 lung adenocarcinomas/large cell carcinomas (7). In this study, NTSR1 (probe set: 207360_s_at) was the 48th among the 58 selected probes related with RFS. NTSR1 was positively regulated. To correlate the NTRS1 transcription level and the RFS over time, a log rank test using the third quartile as the cutoff point was applied to determine high-risk subgroups (Fig. 1). High gene expression for *NTSR1* was associated with an increased risk of relapse ($P = 0.0005$).

Protein expression of neurotensin and NTSR1, and its impact on the survival of patients with primary lung adenocarcinoma

A neurotensin and NTSR1 expression study was done on a multicenter series of 139 consecutive patients undergoing pulmonary lobectomy and nodal dissection for pathologic stage I lung adenocarcinomas. The patient clinical characteristics are shown in Table 1. NTSR1 staining of cancer cells from patients with primary lung adenocarcinoma was granular, restricted to the cytoplasm, and rarely localized at the cell surface (Fig. 2A, left). Neurotensin labeling was often very intense and always detected throughout the cytosol (Fig. 2A, right). Expression of neurotensin, NTSR1, or both was found in 60.4%, 59.7%, and 38.8% of the cases, respectively. Similar results were found when neurotensin and NTSR1 transcripts were studied (23 patients): 65% of patients expressed neurotensin (Fig. 2B, red dots), 69% expressed NTSR1 (Fig. 2B, green dots), and 43% expressed both markers. No expression of either neurotensin or NTSR1 was observed in the lung parenchyma of 26 patients with idiopathic pneumothorax treated by apical resection (Fig. 2A), suggesting that normal lung tissue does not express neurotensin or NTSR1.

The impact of neurotensin/NTSR1 expression on outcome was assessed on 138 of 139 patients, with a patient lost at follow-up. The overall 5-year survival was 63.5% [95% confidence interval (95% CI), 54.4-71.7%]. With respect to those clinical and pathologic parameters influencing

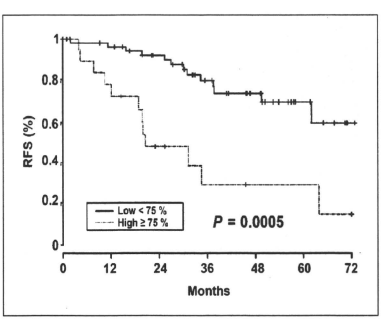

Fig. 1. Relapse-free survival of a study resulting from transcriptome analysis. Large-scale gene expression analysis done on 74 homogeneous cases of stage pT_2N_0 lung adenocarcinomas/large cell carcinomas treated by surgery. Depicted according to the procedure described by Broet et al. (7), the transcriptomic signature of selected positive scores indicates that overexpression increases relapse risk. Shown is the Kaplan-Meier plot according to NTSR1 mRNA levels over (broken line) or below (solid line) the 75th percentile.

DOI:10.1158/1078-0432.CCR-10-0659

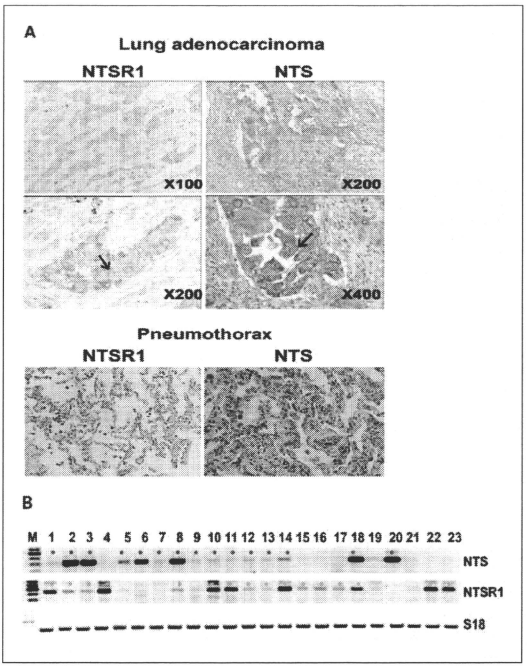

Fig. 2. Neurotensin (NTS) and NTSR1 expression in patients with primary lung adenocarcinomas. A, example of immunohistochemistry for NTSR1 (left) and NTS (right). Top, positive labeling of patients with primary lung adenocarcinomas; bottom, negative labeling of idiopathic pneumothorax at ×200 magnification. B, NTS and NTSR1 transcript analysis on RNA from 23 patients with primary lung adenocarcinomas stage I. M, 100 bp ladder. Patients with red dot or green dot were considered as positive for NTS or NTSR1, respectively.

patient outcome, no difference was observed in survival rates using univariate analysis according to sex, pT parameter, presence of vascular or lymphatic tumoral emboli, or smoking habit (current and former versus never). Five-year survival rates were 72.0% and 57.7% in patients with T_1N_0 and T_2N_0 tumors, respectively ($P = 0.13$). Patients of age 65 years or older had a lower 5-year survival ($P = 0.0028$) as compared with younger patients, at 49.3% (95% CI, 36.2-62.4%) versus 75.9% (95% CI, 64.2-84.7%), respectively. NTSR1 expression, scored as positive (positive staining involving ≥10% of tumor cells) or negative (positive staining of <10% of tumor cells) was associated with a significantly worse 5-year overall survival [54.6% (95% CI, 42.82-65.86%) versus 76.1% (95% CI, 62.4-85.9%); $P = 0.0081$; Fig. 3A]. The degree of NTSR1 expression also significantly influenced outcome ($P = 0.015$), as patients with none (positive staining of <10% of tumor cells), medium (positive staining of ≥10% and <50% of tumor cells), and strong (positive staining involving ≥50% of tumor cells) NTSR1 expression showed 5-year overall survival rates of 76.1% (95% CI, 62.2-86.0%), 56.4% (95% CI, 43.8-68.1%), and 40.5% (95% CI, 15.3-72%), respectively (Fig. 3B). Two independent predictors of worse overall survival were found using multivariate analysis: age ≥65 years ($P = 0.0018$) and expression of NTSR1 ($P = 0.0034$).

NTSR1 expression was also associated with a significantly worse 5-year RFS, at 56.5% (95% CI, 45.5-66.8%) versus 79.3% (95% CI, 65.6-88.5%) in patients with tumors expressing or not expressing NTSR1, respectively ($P = 0.0024$; Fig. 3C). The degree of NTSR1 expression also significantly ($P = 0.0076$) influenced outcome, as patients with none, medium, and strong NTSR1 expression showed 5-year RFS of 79.3% (95% CI, 65.6-88.5%), 57.3% (95% CI, 45.6-68.3%), and 50.0% (95% CI, 23.6-76.3%), respectively (Fig. 3D). Two independent predictors of worse RFS were found using multivariate analysis: expression of NTSR1 ($P = 0.00066$) and age ≥65 years ($P = 0.00142$). In contrast, neurotensin expression in human tumor did influence neither overall survival nor RFS (Supplementary Fig. S1).

DOI:10.1158/1078-0432.CCR-10-0659

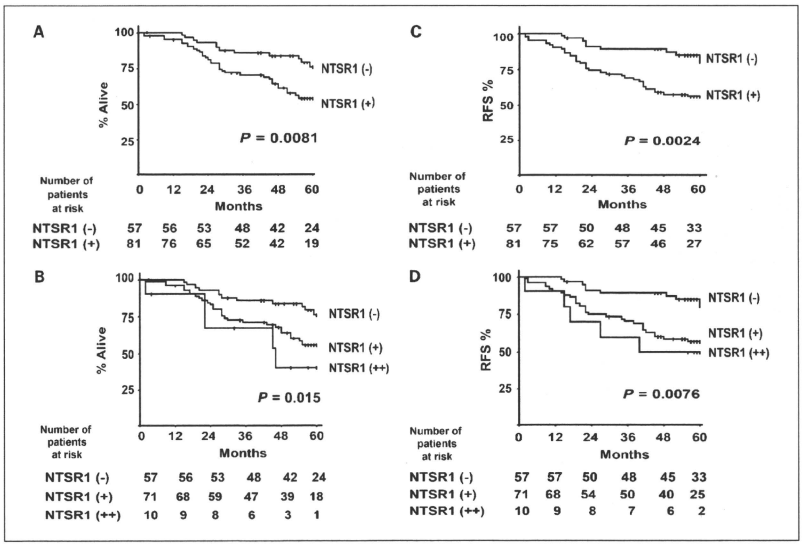

Fig. 3. Overall survival and RFS of patients with stage I adenocarcinoma (n = 138) according to NTSR1 expression. A and C, qualitative assessment by immunohistochemistry of NTSR1 expression: (+), positive; (-), negative. B and D, semiquantitative immunohistochemistry: (++), strong expression; (+), medium expression; (-), no expression. The number of patients at risk for each time period is shown below each curve.

Influence of the neurotensin/NTSR1 signaling system on the tumorigenic potential of human lung cancer cells

To evaluate the role of the neurotensin/NTSR1 complex in tumor growth and progression, we used mice xenografted with cancer cells expressing or not expressing the neurotensin/NTSR1 system. We first established xenografts from the adenocarcinoma cell line A549. As shown in Fig. 4A (inset), this cell line expressed both neurotensin and NTSR1. The silencing of NTSR1 induced a 40% reduction in the growth of tumor xenografts in nude mice compared with wild-type cells (Fig. 4A).

Additional evidence of the impact of the neurotensin system on tumor growth derived from LNM-R, a subpopulation of the highly metastatic lung carcinoma cell line LNM35 (23). LNM-R cells express neurotensin and NTSR1 as shown by transcript analysis (Fig. 4B, inset). Experimental lung tumors were generated using LNM-R cells and the silenced derivative clones R-SI NTS and R-SI NTSR1. In the clone R-S1 NTS, the transcript encoding neurotensin was completely depleted (Fig. 4B, inset). This result was confirmed by the absence of neurotensin estimated by RIA on the corresponding culture media. In contrast, the culture medium of LNM-R cells contained 76.4 ± 10.3, 153.2 ± 25.3, and 624.3 ± 81.8 fmol/mL of neurotensin corresponding to 14, 48, and 72 hours of culture, respectively. In the clone R-SI NTSR1, the transcript for NTSR1 was depleted, whereas neurotensin transcript levels remained similar to those of LMN-R cells. An example is shown in the inset of Fig. 4B. The level of neurotensin released in the culture media was lower than for LNM-R cells at 22.25 ± 2.4, 53.4 ± 2.7, and 140.2 ± 9 fmol/mL corresponding to 14, 48, and 72 hours of culture, respectively.

Using these models, we examined the effect of neurotensin and NTSR1 depletion on the growth of LNM-R xenografts and their neurotensin- and NTSR1-silenced counterparts. Depletion of neurotensin and NTSR1 was accompanied respectively by 35% and 60% decrease of the tumor volume compared with the LNM-R tumor xenografts at day 28 (Fig. 4B). To show the participation of neurotensin in tumor growth enhancement, a mixture of the two silenced clones was seeded at equal density (50/50) and cultured for 3 days, prior to injection into mice. The final tumor volume and weight were similar to those of the parental LNM-R tumor xenografts. Together these results strengthen the tumorigenic consequence of neurotensin

DOI:10.1158/1078-0432.CCR-10-0659

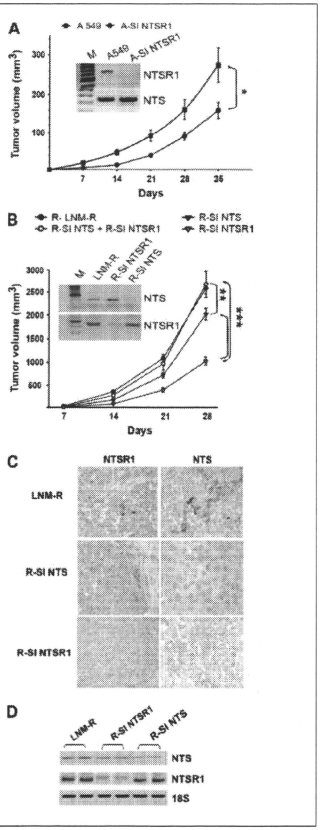

Fig. 4. Tumor growth generated by the human lung adenocarcinoma cell lines. A, A549 cells, or its NTSR1-silenced clone A-SI NTSR1 were injected into 15 mice for each cell line. Inset, NTS and NTSR1 transcript analysis on A549 cells, and A-SI NTSR1 RNA. *, significant differences at $P < 0.05$, using unpaired t test. B, LNM-R, R-SI NTS, R-SI NTSR1, or a 50/50 mixture of R-SI NTS and R-SI NTSR1 cells were injected into 36, 21, 21, and 19 mice, respectively. The ellipsoid formula was used to calculate the volume. Inset, NTS and NTSR1 transcripts analysis on total RNA from LNM-R, R-SI NTSR1, and R-SI NTS. C, typical immunohistochemistry for NTSR1 (left) or NTS (right) for tumors generated from R-SI NTS (top) or R-SI NTSR1 cells (bottom). D, NTS and NTSR1 transcript analysis on tumors from LMN-R, R-SI NTSR1, and R-SI NTS cells. Analysis was done at day 28. Examples of two different tumors are shown. ***, significant differences at $P < 0.001$; **, at $P < 0.01$ using ANOVA and Student-Neuman-Keuls test.

autocrine or paracrine regulation (Fig. 4B). A similar pattern was observed in tumor weight with 4 ± 0.2, 2.8 ± 0.18, 1.54 ± 0.17, and. 3.4 ± 0.16 g for LNM-R, R-SI NTS, R-SI NTSR1, and the 50/50 R-SI NTS/R-SI NTSR1 cellular mixture, respectively. Neurotensin and NTSR1 immunohistochemistry and transcript analysis on tumor xenografts shows that neurotensin and NTSR1 silencing constructs were still efficient at 28 days postinjection (Fig. 4C and D).

Influence of the neurotensin/NTSR1 complex on nodal metastasis

The ipsilateral and controlateral regional lymph nodes from mice bearing either LNM-R or the silenced clones for neurotensin and NTRS1 were dissected. The weight of the lymph nodes was 2.5 times smaller when the tumor was not expressing neurotensin or NTSR1 (Fig. 5A). Metastases were scored by an anatomopathologist as negative, micro (metastases <1 mm), and massive (Fig. 5B). After 28 days, mice bearing tumor R-SI NTS and R-SI NTSR1 xenografts had a smaller percentage of massively invaded lymph nodes (9% and 24%, respectively), as compared with 66% for the LNM-R xenografts ($P < 0.0001$ and $P = 0.0047$, respectively, Fisher's exact test; Fig. 5C). The respective distribution of negative, micro, and massive lymph node metastasis is detailed under the graph in Fig. 5C. The negative and the micro metastasis were combined to form a single set because it covers the global effect of neurotensin/NTSR1 on metastatic process.

Discussion

In this study we found that NTSR1 and neurotensin were not detected in normal pulmonary tissue, but were strongly and frequently expressed in stage I lung adenocarcinomas. Similar results have been seen in colon and breast tissues where NTSR1 is absent in normal epithelial cells but overexpressed in tumors (20, 26). As previously described, one of the possible molecular mechanisms responsible for NTSR1 upregulation is the *Wnt*/APC signaling pathway activation, because of a functional Tcf element within the NTSR1 promoter. In normal human breast epithelial cells, the activation of the *NTSR1* gene was observed by agents causing β-catenin cytosolic accumulation (15). A set of TCF4 regulated genes was recently shown to be associated with metastasis-free survival in patients with lung adenocarcinoma (27). In this study, the transcription factors HOXB9 and LEF1 were identified as mediators of chemotactic invasion. Accordingly, a hyperactive Wnt/TCF pathway activity in lung adenocarcinomas is associated with a high rate of relapse at distant sites. As part of Wnt/Tcf activated genes, *NTSR1* should participate in disease progression and correlation with the worst prognosis.

The availability of useful prognostic factors in NSCLC is made difficult because of the extreme heterogeneity in patient populations in terms of histologic typing, disease staging, type of surgical treatment, and the association with neoadjuvant or adjuvant therapy. For these reasons, we focused our study on patients with stage I primary lung

DOI:10.1158/1078-0432.CCR-10-0659

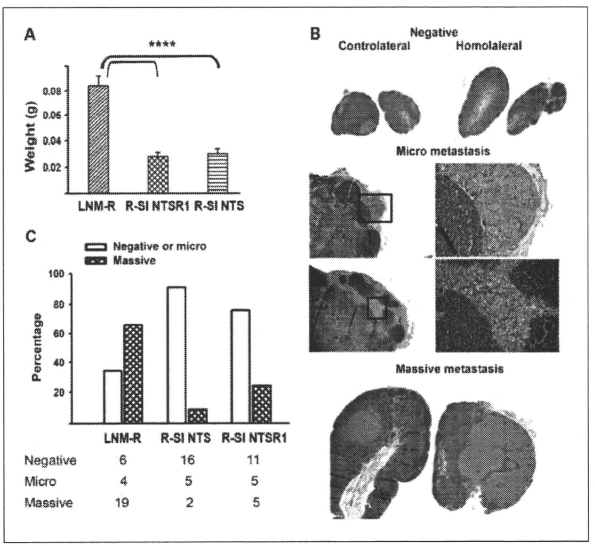

Fig. 5. Lymph node metastasis generated by lung cancer cell lines LNM-R and their subclonal counterparts silenced for NTS and NTSR1. A, ipsilateral lymph node weight at 28 days form mice xenografted with LMN-R, R-SI NTSR1, and R-SI NTS cells. ***, significant differences at $P < 0.001$ using ANOVA and Student-Neuman-Keuls test. B, standard H&E staining done on paraffin section of lymph node embedded tissue. Example is shown for negative (top); micro metastasis, less than 1 mm (middle); and massive metastasis (bottom) of homolateral lymph node. C, for each group, the percentage of ipsilateral lymph nodes with no and micro metastasis or with massive metastasis, from mice xenografted with LMN-R, R-SI NTSR1, and R-SI NTS cells, at 29, 21, and 23 mice, respectively.

adenocarcinoma, treated by surgery only (pulmonary lobectomy and full nodal dissection). This ensured the reliability of the staging and the absence of interfering treatments.

In our clinical series from 138 homogeneous patients with stage I disease, NTSR1 expression was correlated with poor outcome. This result was confirmed by multivariate analysis which showed that among the available clinical and pathologic factors, only the expression of NTSR1 and patient age were independent predictors of worse prognosis. These findings in human lung cancer suggest that NTSR1 is a potential marker and/or a pejorative mediator of lung cancer progression associated with poor prognosis.

In contrast, no correlation was found between neurotensin expression and patient survival. Neurotensin expression in the lung tumor is certainly part of the neoplastic process but is not a discriminative factor of disease progression. The molecular mechanism inducing neurotensin expression in lung neoplasm remains unclear. As it was shown that neurotensin expression can be upregulated by inflammatory process and mediates proinflammatory cytokine release, such as interleukin-6 and interleukin-8 (28, 29), we propose that neurotensin expression is induced and implicated in the pathogenesis of lung cancer due to chronic inflammation and neoplasia in the respiratory epithelium generated by tobacco carcinogens and metabolites. The evaluation of neurotensin expression in premalignant lesions will settle this hypothesis.

To delineate the biological significance of the neurotensin/NTSR1 system in the progression of human lung tumors, we studied the performance of the neurotensin/NTSR1 complex on tumor growth and progression. Removing neurotensin sensitivity and NTSR1 signaling resulted in a strong reduction of lung cancer cell proliferation and tumor growth in the two experimental models. The silencing of neurotensin was less efficient than NTSR1 silencing in negating the growth of the LNM-R xenografts, suggesting that circulating neurotensin in mice may counteract the depletion of neurotensin induced by RNA interference in cancer cells. Substantiating this argument, we noted that when R-SI NTSR1 cells were injected s.c. into the right flank and R-SI NTS cells in the left flank of the mice, the latter tumor reach the size and weight of the tumors initiated by the corresponding LMN-R parental cells; in contrast, R-SI NTSR1 tumors remained at the same smaller size that was observed in mice bearing only R-SI NTSR1 xenografts (unpublished data). It is likely that neurotensin systemic regulation is implicated in the growth of the tumor xenografts.

Our data support the position that LNM-R cancer cells are driven by an autocrine neurotensin-NTSR1 loop to incur invasive tumor growth and metastasis. LNM-R is a subpopulation of LNM-35 cells selected for their metastatic

DOI:10.1158/1078-0432.CCR-10-0659

properties (23). Within the time period of the experiments, 70% of mice bearing LNM-R xenografts exhibited massive lymph node metastasis. The invalidation of the neurotensin/NTSR1 system in LNM-R cells was associated with less aggressive primary tumor xenografts, and it restricted the metastatic process. Once the cells acquire metastatic potential, the presence of neurotensin in the tumor microenvironment potentiates the emergence of metastasis. When replaced in the context of stage I patients with adenocarcinoma, most of these patients are treated only with surgery as adjuvant treatment, which has not been shown to improve the global outcome (30). In these patients, local and distant tumor recurrence should arise either from active or dormant cancer cells that have spread, both kinds being undetectable with the current diagnostic methods (31). Our experimental model predicts that the autocrine or paracrine loop involved in NTSR1 activation in those patients would enhance tumor progression and recurrence.

Patients within the initial stages of NSCLC are best managed by surgery, with no consensus existing regarding postoperative follow-up measures (32). The identification of patients with poor prognosis, within a determined stage, would be of major importance for the management of patients with NSCLC (33), as the follow-up procedures could be individually tailored. Furthermore, patients with poor prognosis, within a determined stage, could be identified as more suitable candidates for postoperative treatments. Adjuvant chemotherapy has been shown to improve the prognosis of patients with stage II-IIIa resected NSCLC, whereas no benefit has been observed in patients with stage Ia, and the results remain controversial in stage Ib (30). Thus, in patients with stage Ib, the identification of a good prognosis marker would represent an important element permitting the avoidance of adjuvant chemotherapy.

Our data indicate that the neurotensin/NTSR1 system is a good prognostic marker useful to identify, within stage I disease patients, those with a bad prognosis. Furthermore, the role of neurotensin in the growth of experimental tumors would represent a basis for the development of specifically targeted drugs, to be used together with currently available treatments.

Disclosure of Potential Conflicts of Interest

No potential conflicts of interest were disclosed.

Acknowledgments

We thank Dr. Ferec for microsatellite analysis of the LNM35 and its subclones and Dr. Neil Insdorf for his helpful discussions and editing.

Grant Support

INSERM and Grants from ARC: 3543, and 3905, "Ligue contre le Cancer" 07/75-85, GEFLUC, and MERLION (5-07-06). S. Dupouy was supported by the "Ligue contre le cancer," M. Younes was supported by Damas University, and S.M. Ahmed Zaid was supported by PHYWE Systeme GmbH und Co. KG.

The costs of publication of this article were defrayed in part by the payment of page charges. This article must therefore be hereby marked *advertisement* in accordance with 18 U.S.C. Section 1734 solely to indicate this fact.

Received 03/17/2010; revised 06/16/2010; accepted 06/27/2010; published online 09/01/2010.

References

1. Alberg AJ, Ford JG, Samet JM. Epidemiology of lung cancer: ACCP evidence-based clinical practice guidelines. Chest 2007;132: 29–55S.
2. Edwards BK, Brown ML, Wingo PA, et al. Annual report to the nation on the status of cancer, 1975–2002, featuring population-based trends in cancer treatment. J Natl Cancer Inst 2005;97:1407–27.
3. Parkin DM, Bray F, Ferlay J, Pisani P. Global cancer statistics, 2002. CA Cancer J Clin 2005;55:74–108.
4. Goldstraw P, Crowley J, Chansky K, et al. The IASLC Lung Cancer Staging Project: proposals for the revision of the TNM stage groupings in the forthcoming (seventh) edition of the TNM Classification of malignant tumours. J Thorac Oncol 2007;2:706–14.
5. Mountain CF, Dresler CM. Regional lymph node classification for lung cancer staging. Chest 1997;111:1718–23.
6. Mountain CF. Revisions in the International System for Staging Lung Cancer. Chest 1997;111:1710–7.
7. Broet P, Camilleri-Broet S, Zhang S, et al. Prediction of clinical outcome in multiple lung cancer cohorts by integrative genomics: implications for chemotherapy selection. Cancer Res 2009;69:1055–62.
8. Reinecke M. Neurotensin. Immunohistochemical localization in central and peripheral nervous system and in endocrine cells and its functional role as neurotransmitter and endocrine hormone. Prog Histochem Cytochem 1985;16:1–172.
9. Baca I, Feurle GE, Schwab A, Mittmann U, Knauf W, Lehnert T. Effect of neurotensin on exocrine pancreatic secretion in dogs. Digestion 1982;23:174–83.
10. Andersson S, Rosell S, Hjelmquist U, Chang D, Folkers K. Inhibition of gastric and intestinal motor activity in dogs by (Gln4) neurotensin. Acta Physiol Scand 1977;100:231–5.
11. Zhao D, Pothoulakis C. Rho GTPases as therapeutic targets for the treatment of inflammatory diseases. Expert Opin Ther Targets 2003; 7:583–92.
12. Leyton J, Garcia-Marin L, Jensen RT, Moody TW. Neurotensin causes tyrosine phosphorylation of focal adhesion kinase in lung cancer cells. Eur J Pharmacol 2002;442:179–86.
13. Ehlers RA, Zhang Y, Hellmich MR, Evers BM. Neurotensin-mediated activation of MAPK pathways and AP-1 binding in the human pancreatic cancer cell line, MIA PaCa-2. Biochem Biophys Res Commun 2000;269:704–8.
14. Moody TW, Chiles J, Casibang M, Moody E, Chan D, Davis TP. SR48692 is a neurotensin receptor antagonist which inhibits the growth of small cell lung cancer cells. Peptides 2001;22:109–15.
15. Souaze F, Viardot-Foucault V, Roullet N, et al. Neurotensin receptor 1 gene activation by the Tcf/β-catenin pathway is an early event in human colonic adenomas. Carcinogenesis 2006;27:708–16.
16. Maoret JJ, Anini Y, Rouyer-Fessard C, Gully D, Laburthe M. Neurotensin and a non-peptide neurotensin receptor antagonist control human colon cancer cell growth in cell culture and in cells xenografted into nude mice. Int J Cancer 1999;80:448–54.
17. Toy-Miou-Leong M, Cortes CL, Beaudet A, Rostene W, Forgez P. Receptor trafficking via the perinuclear recycling compartment accompanied by cell division is necessary for permanent neurotensin cell sensitization and leads to chronic mitogen-activated protein kinase activation. J Biol Chem 2004;279:12636–46.

DOI:10.1158/1078-0432.CCR-10-0659

18. Najimi M, Souaze F, Mendez M, et al. Activation of receptor gene transcription is required to maintain cell sensitization after agonist exposure. Study on neurotensin receptor. J Biol Chem 1998;273:21634–41.
19. Somai S, Gompel A, Rostene W, Forgez P. Neurotensin counteracts apoptosis in breast cancer cells. Biochem Biophys Res Commun 2002;295:482–8.
20. Souaze F, Dupouy S, Viardot-Foucault V, et al. Expression of neurotensin and NT1 receptor in human breast cancer: a potential role in tumor progression. Cancer Res 2006;66:6243–9.
21. Shimizu S, Tsukada J, Sugimoto T, et al. Identification of a novel therapeutic target for head and neck squamous cell carcinomas: a role for the neurotensin-neurotensin receptor 1 oncogenic signaling pathway. Int J Cancer 2008;123:1816–23.
22. Dupouy S, Viardot-Foucault V, Alifano M, et al. The neurotensin receptor-1 pathway contributes to human ductal breast cancer progression. PLoS ONE 2009;4:e4223.
23. Kozaki K, Miyaishi O, Tsukamoto T, et al. Establishment and characterization of a human lung cancer cell line NCI-H460-LNM35 with consistent lymphogenous metastasis via both subcutaneous and orthotopic propagation. Cancer Res 2000;60:2535–40.
24. Souaze F, Rostene W, Forgez P. Neurotensin agonist induces differential regulation of neurotensin receptor mRNA. Identification of distinct transcriptional and post-transcriptional mechanisms. J Biol Chem 1997;272:10087–94.
25. Scarceriaux V, Pelaprat D, Forgez P, Lhiaubet AM, Rostene W. Effects of dexamethasone and forskolin on neurotensin production in rat hypothalamic cultures. Endocrinology 1995;136:2554–60.
26. Maoret JJ, Pospai D, Rouyer-Fessard C, et al. Neurotensin receptor and its mRNA are expressed in many human colon cancer cell lines but not in normal colonic epithelium: binding studies and RT-PCR experiments. Biochem Biophys Res Commun 1994;203:465–71.
27. Nguyen DX, Chiang AC, Zhang XH, et al. WNT/TCF signaling through LEF1 and HOXB9 mediates lung adenocarcinoma metastasis. Cell 2009;138:51–62.
28. Koon HW, Kim YS, Xu H, et al. Neurotensin induces IL-6 secretion in mouse preadipocytes and adipose tissues during 2,4,6,-trinitrobenzensulphonic acid-induced colitis. Proc Natl Acad Sci U S A 2009;106:8766–71.
29. Zhao D, Zhan Y, Zeng H, Koon HW, Moyer MP, Pothoulakis C. Neurotensin stimulates interleukin-8 expression through modulation of I κ B α phosphorylation and p65 transcriptional activity: involvement of protein kinase C α. Mol Pharmacol 2005;67:2025–31.
30. Wakelee HA, Schiller JH, Gandara DR. Current status of adjuvant chemotherapy for stage IB non-small-cell lung cancer: implications for the New Intergroup Trial. Clin Lung Cancer 2006;8:18–21.
31. Hecht SS. Tobacco smoke carcinogens and lung cancer. J Natl Cancer Inst 1999;91:1194–210.
32. Rubins J, Unger M, Colice GL. Follow-up and surveillance of the lung cancer patient following curative intent therapy: ACCP evidence-based clinical practice guideline. Chest 2007;132:355–67S.
33. Lu Y, Lemon W, Liu PY, et al. A gene expression signature predicts survival of patients with stage I non-small cell lung cancer. PLoS Med 2006;3:e467.

The American Journal of Pathology, Vol. 176, No. 4, April 2010

DOI: 10.2353/ajpath.2010.090829

Tumorigenesis and Neoplastic Progression

Endogenous Angiogenesis Inhibitor Vasohibin1 Exhibits Broad-Spectrum Antilymphangiogenic Activity and Suppresses Lymph Node Metastasis

Takahiro Heishi,* Tomoko Hosaka,* Yasuhiro Suzuki,* Hiroki Miyashita,* Yuichi Oike,† Takashi Takahashi,‡ Takumi Nakamura,§ Shingo Arioka,§ Yuichi Mitsuda,§ Tomoaki Takakura,§ Kanji Hojo,§ Mitsunobu Matsumoto,§ Chihiro Yamauchi,§ Hideki Ohta,§ Hikaru Sonoda,§ and Yasufumi Sato*

From the Department of Vascular Biology, Institute of Development, Aging, and Cancer, Tohoku University, Sendai; the Department of Molecular Genetics,† Graduate School of Medical Sciences, Kumamoto University, Kumamoto; the Division of Molecular Carcinogenesis,‡ Center for Neurological Diseases and Cancer, Nagoya University Graduate School of Medicine, Nagoya; and the Discovery Research Laboratories,§ Shionogi & Co. Ltd., Osaka, Japan*

During cancer progression, the angiogenesis that occurs is involved in tumor growth and hematogenous-distant metastasis, whereas lymphangiogenesis is involved in regional lymph node metastasis. Angiogenesis is counterregulated by various endogenous inhibitors; however, little is known about endogenous inhibitors of lymphangiogenesis. We recently isolated vasohibin1 as an angiogenesis inhibitor intrinsic to the endothelium and further demonstrated its anticancer activity through angiogenesis inhibition. Here, we examined the effect of vasohibin1 on lymphangiogenesis. Vasohibin1 exhibited broad-spectrum antilymphangiogenic activity in the mouse cornea induced by factors including VEGF-A, VEGF-C, FGF2, and PDGF-BB. We then inoculated highly lymph node–metastatic cancer cells into mice and examined the effect of vasohibin1 on lymph node metastasis. Tail-vein injection of adenovirus containing the human *vasohibin1* gene inhibited tumor lymphangiogenesis and regional lymph node metastasis. Moreover, local injection of recombinant vasohibin1 inhibited lymph node metastasis. These results suggest vasohibin1 to be the first known intrinsic factor having broad-spectrum antilymphangiogenic activity and indicate that it suppresses lymph node metastasis. ***(Am J Pathol 2010, 176:1950–1958; DOI: 10.2353/ajpath.2010.090829)***

Peripheral lymphatic vessels, which are composed of a single layer of lymphatic endothelial cells (LECs) without mural cell coverage, collect fluid lost from blood vessels and maintain immune responses, lipid uptake, and tissue homeostasis.[1] Recently, attention has focused on lymphangiogenesis, which is the formation of new lymphatic vessels, because it has been shown to be related to lymph node (LN) metastasis of cancers.[2] Metastasis of malignant tumors to regional LNs is one of the early signs of spreading cancer, and it occurs as frequently as hematogenous distant metastasis.[3]

The formation of blood and lymphatic vessels is primarily controlled by vascular endothelial growth factor (VEGF) family members.[4] This family of growth factors consists of 5 members (ie, VEGF-A, VEGF-B, VEGF-C, VEGF-D, and placental growth factor). There are also 3 types of VEGF receptor (VEGFR) tyrosine kinases: VEGFR1, VEGFR2, and VEGFR3. The most important molecule in the VEGF family that mediates angiogenesis of the formation of new blood vessels is VEGF-A, and VEGFR2 is the major mediator of VEGF-A–driven responses in blood endothelial cells (BECs). Alternatively, the most important factors that mediate lymphangiogenesis are VEGF-C and VEGF-D, and VEGFR3 is the major mediator of VEGF-C– and VEGF-D–mediated responses in LECs.[4] In addition, several factors such as fibroblast growth factor (FGF)2, platele-derived growth factor BB (PDGF-BB), insulin-like growth factor 1

Supported by a grant from the program Grants-in-Aid for Scientific Research on Priority Areas from the Japanese Ministry of Education, Science, Sports, and Culture; by Health and Labor Sciences research grants; and by funding from Third Term Comprehensive Control Research for Cancer from the Ministry of Health, Labor, and Welfare (Japan).

Accepted for publication December 11, 2009.

Address reprint requests to Yasufumi Sato, M.D., Ph., Department of Vascular Biology, Institute of Development, Aging, and Cancer, Tohoku University, 4-1, Seiryo-machi, Aoba-ku, Sendai 980-8575, Japan. E-mail: y-sato@idac. tohoku.ac.jp.

(IGF1), and hepatocyte growth factor (HGF) are reported to induce both angiogenesis and lymphangiogenesis.[5–8]

Angiogenesis is counterbalanced by various endogenous inhibitors.[9] However, little is known about endogenous inhibitors of lymphangiogenesis. Thrombospondin 1 (TSP1), an angiogenesis inhibitor, does not inhibit lymphangiogenesis.[10] Endostatin, another angiogenesis inhibitor, inhibits lymphangiogenesis and LN metastasis of certain tumors, but its effect on lymphangiogenesis is mediated via the down-regulation of VEGF-C in tumor cells.[11,12]

Recently, while searching for novel and functional VEGF-A–inducible molecules in endothelial cells (ECs), we identified an intrinsic inhibitor of angiogenesis in the vascular endothelium and named it vasohibin (VASH).[13] Thereafter we isolated a homologue of VASH, and so we designated it as VASH2 and renamed the original VASH as VASH1.[14] Our subsequent analysis revealed that VASH1 is expressed in BECs in the termination zone to halt angiogenesis, whereas VASH2 is expressed in infiltrating mononuclear cells in the sprouting front to promote angiogenesis.[15] When applied exogenously, VASH1 effectively inhibits various kinds of pathological angiogenesis[13,16–18] and inhibits tumor growth.[13,18] Here, we examined whether VASH1 has any effect on lymphangiogenesis, and if so, on LN metastasis of tumors. Our present study provides evidence that intrinsic factor VASH1 exhibited broad-spectrum antilymphangiogenic activity and inhibited LN metastasis.

Materials and Methods

All of the animal studies were reviewed and approved by the committee for animal study at our institute in accord with established standards of humane handling of research animals.

Mouse Corneal Micropocket Assay

Mouse corneal micropocket assays were performed as described previously.[13] Briefly, 4-week-old male BALB/c mice (Charles River Laboratories Japan, Inc., Yokohama, Japan) were deeply anesthetized, and 0.3 μg of poly-2-hydroxyethyl methacrylate (HEME) pellets (Sigma, St. Louis, Mo, USA) containing either vehicle or 160 ng of VEGF-A ($VEGF_{165}$, Sigma), 160 ng of VEGF-$C_{Cys156ser}$ (R&D Systems, Inc., Minneapolis, MN), 12.5 ng or 80 ng of FGF2 (BD Biosciences, San Jose, CA), or 80 ng of PDGF-BB (R&D Systems, Inc.) was implanted in the corneas. A total of 4 ng of VASH1 protein was added or not to the pellets.

Fourteen days after the pellet inoculation, the corneas were excised, washed in PBS, and fixed in acetone at 4°C for 30 minutes. After three additional washings in PBS and blocking with 1% BSA in PBS for 1 hour, the corneas were stained overnight at 4°C with rabbit anti-mouse lymphatic vessel endothelial receptor 1 (LYVE1) antibody (1:500; Acris Antibodies GmbH, Hiddenhausen, Germany) and rat anti-mouse CD31 antibody (1:500; Research Diagnostics Inc., Flanders, NJ). On day 2, the corneas were washed, and secondary antibody reactions were performed by treatment with Alexa Fluor 488-conjugated donkey anti-rat IgG (1:1000; Invitrogen Corp., Carlsbad, CA) and Alexa Fluor 568-conjugated goat anti-rabbit IgG (1:1000; Invitrogen Corp.) for 6 hours at 4°C. After a last washing, the sections were covered with fluorescence mounting medium (DakoCytomation Inc., Carpinteria, CA). Double-stained whole-mount sections were observed under a FluoView FV1000 confocal microscope (Olympus Corp., Tokyo, Japan). Blood vessels were positive for CD31 antigen, and lymphatic vessels were positive for LYVE1. The area covered by blood and lymphatic vessels was measured by using NIH ImageJ software (v. 1.39u).

Subcutaneous Tumor Xenograft Model

Cells of the human lung cancer cell line NCI-H460-LNM35 (LNM35, 1.0×10^7 cells) were implanted into the subcutaneous tissue of the right abdominal wall of female SCID mice (6 to 8 weeks old, Charles River Laboratories, Japan). A replication-defective adenovirus vector encoding human *vasohibin1* (AdVASH1) or *β-galactosidase* gene (AdLacZ, 1×10^9 plaque-forming units [pfu]) was intravenously injected into a tail vein at day 0 and day 14 after the implantation.[17] Four weeks after the inoculation the mice were sacrificed, and tumors, along with some internal organs such as the trachea and axillary LNs, were collected. The sizes of axillary LNs were measured, and sections of the nodes were stained with hematoxylin and eosin to evaluate tumor metastasis.

Tissues were embedded in optimal cutting temperature (OCT) compound (Sakura Finetechnical, Tokyo, Japan) to make frozen tissue specimens, and sectioned at 6 μm. Samples were fixed with methanol for 20 minutes at −20°C, blocked with 1% BSA in PBS for 30 minutes at room temperature, and stained with anti-mouse LYVE-1 antibody (1:500), anti-mouse CD31 antibody (1:500), or anti-mouse F4/80 antibody (1:500; Acris Antibodies GmbH) at 4°C overnight. This action was followed by staining with secondary antibodies Alexa fluor 488 donkey anti-rat IgG (1:1000), Alexa fluor 568 goat anti-rabbit IgG (1:1000) and TO-PRO-3 iodide (1:1000; Invitrogen Corp.) for 30 minutes at room temperature. After having been washed three times with PBS, the sections were covered with fluorescence mounting medium and observed under an Olympus FluoView FV1000 confocal microscope. The vascular lumen was traced, and the vascular luminal area was analyzed with NIH ImageJ software.

Western Blotting of Human VASH1 Protein

Frozen tissues (vena cava, kidney, liver, lung, and heart) were homogenized and lysed with modified RIPA buffer. Mouse blood was heparinized and centrifuged to obtain plasma. Albumin and IgG were depleted from the plasma with a removal kit according to the manufacturer's protocol (Amersham Biosciences Corp., Piscataway, NJ). Thereafter, Western blot analysis was performed as described previously.[13] Horseradish peroxidase (HRP)-labeled anti-human VASH1 monoclonal antibody (clone 4E12) was used, which recognized human but not murine VASH1 protein.

ELISA for VASH1

Peptides corresponding to Gly286-Arg299 (VC1) and Ala217-Lys229 (VR) of human VASH1 protein were conjugated with keyhole limpet hemocyanin. These antigens were used to immunize A/J mice, and several monoclonal antibodies were prepared as described previously.[13] We examined various combinations of monoclonal antibodies and found that the combination of VC1-derived clone 12F6 and VR-derived clone 12E7 was ideal for a highly sensitive and specific ELISA system that could detect human and mouse VASH1 protein equally. We used 12F6 and 12E7 for plate coating and HRP labeling, respectively. The detailed procedure for the measurement was described previously.[19]

Preparation of Recombinant VASH1 Protein

Human *VASH1* gene with optimized codons for *Escherichia coli* (*E. coli*) expression was cloned in pET-32 LIC/Xa (Novagen, Madison, WI). The resultant expression plasmid encoded *VASH1* with a sequence of GSNSPLAMAISDPNSSSVDKLAAALEHHHHHH at its C terminus. *E. coli* transformants were cultivated at 37°C in TB (2.4 M yeast extract, 1.2 Mtryptone, 1.25 M K_2HPO_4, 0.23 M KH_2PO_4, 500 μg/ml polypropylene glycol #2000, 50 μg/ml ampicillin; pH 7.0) supplied with 4% glycerol, and the expression was induced by the addition of 1 mmol/L isopropyl β-D-1-thiogalactopyranoside (OD_{650} = 5). After a 16-hour cultivation, cells were collected and disrupted in 20 mmol/L sodium phosphate buffer, pH 7.6, containing 0.5 mol/L NaCl and 1 mmol/L phenylmethylsulfonyl fluoride in a high-pressure homogenizer. The inclusion bodies were collected, washed with the same buffer, and solubilized in 20 mmol/L sodium phosphate buffer, pH 8.0, containing 0.5 mol/L NaCl, 1 mmol/L phenylmethylsulfonyl fluoride, 5 mmol/L 2-mercaptoethanol, 60 mmol/L imidazole, and 7 mol/L guanidine-HCl. The soluble fraction was loaded onto a Ni Chelating Sepharose column (16 mm × 125 mm, GE health care, Carnegie Center, NJ) equilibrated with the above solubilization buffer except that the guanidine-HCl was replaced by 8 mol/L urea and eluted with the same buffer containing 300 mmol/L imidazole. VASH1 fusion protein fraction was dialyzed against 20 mmol/L glycine-HCl buffer, pH 3.5, and digested with coagulation factor Xa (Novagen) for 1 hour at

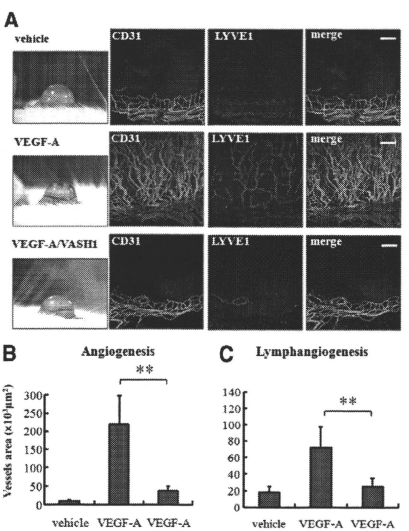

Figure 1. VASH1 inhibits angiogenesis and lymphangiogenesis induced by VEGF-A. **A:** Pellets containing 160 ng of VEGF-A plus or minus 4 ng of VASH1 were inoculated into the mouse cornea. Fourteen days after the inoculation, the corneas were harvested and immunostained for LYVE1 (red) or CD31 (green). Scale bar = 200 μm. Experiments were repeated at least 3 times, and representative data are shown here. **B:** The area of CD31-positive vessel was quantified; the means and SDs are shown. VASH1 significantly inhibited angiogenesis and lymphangiogenesis induced by VEGF-A. $n = 5$, $^{**}P < 0.01$. **C:** The area occupied by LYVE1-positive vessel was quantified, and the means and SDs shown. VASH1 significantly inhibited the lymphangiogenesis induced by VEGF-A. $n = 5$, $^{**}P < 0.01$.

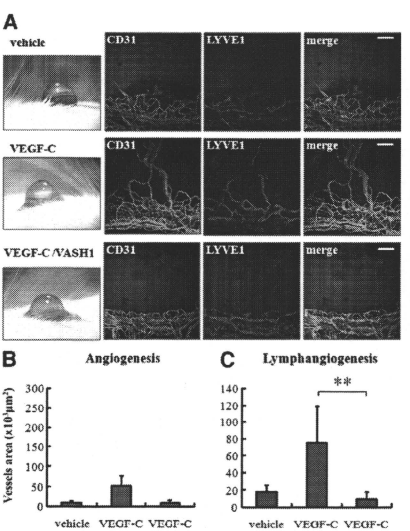

Figure 2. VASH1 inhibits angiogenesis and lymphangiogenesis induced by VEGF-C. **A:** Pellets containing 160 ng of VEGF-C plus or minus 4 ng of VASH1 were inoculated into the mouse cornea. Fourteen days after the inoculation, corneas were harvested and immunostained for LYVE1 or CD31. Scale bar = 200 μm. Experiments were repeated at least 3 times, and representative data are shown here. **B:** The area of CD31-positive vessel was quantified, and the means and SDs are shown. VEGF-C limitedly stimulated angiogenesis, as did VASH1, though no significant differences were observed. $n = 5$. **C:** The area of LYVE1-positive vessels was quantified, and the means and SDs are shown. VASH1 significantly inhibited the lymphangiogenesis induced by VEGF-C. $n = 5$, $^{**}P < 0.01$.

25°C. The released VASH1 protein was collected, solubilized, and purified with Ni Chelating Sepharose. VASH1 protein was then collected as the insoluble fraction after dialysis against 20 mmol/L Tris-HCl (pH 8.0), resolubilized in 25 mmol/L sodium phosphate (pH 7.2) containing 4 mol/L urea, loaded onto a Q Sepharose column (16 mm × 140 mm, GE health care), and eluted by linearly increasing the NaCl concentration to 1 mol/L. Finally, the VASH1 protein was dialyzed against 20 mmol/L glycine-HCl buffer (pH 3.5).

Orthotopic Tumor Xenograft Model

Human breast cancer cell line MDA-MB-231 obtained from American Type Culture Collection was transfected with firefly luciferase and geneticin resistance genes, and stable transfectants (231Luc-1 cells) were selected. 231Luc-1 cells were inoculated into the mammary fat pad of mice, and spontaneous LN metastatic cells (231LN-Luc-1 cells) were isolated from the axillary LNs and cultured.

231LN-Luc-1 cells (5×10^6) in 50 μl of 40% Hanks' balanced salt solution containing 50% Matrigel (Becton, Dickinson and Company, Franklin Lakes, NJ) and 10% VASH1 or human serum albumin (HSA) solution (5 μg protein/50 μl solution) were inoculated into the abdominal mammary fat pad of female C57BL-17/Icr SCID Jcl mice (CLEA Japan, Inc., Tokyo, Japan). Six days after the inoculation, 2.5 μg of VASH1 or HSA was locally injected into the abdominal mammary fat pad every 3 to 4 days. LN metastasis (axillary region) was analyzed on day 32 by a bioluminescence imaging technique. Fifty to 60 seconds after the luciferin injection, mice were placed in the IVIS Imaging System (Xenogen, Alameda, CA) and imaged. LN metastasis was quantified as photons/sec obtained with Living Image® software (Xenogen).

Calculations and Statistical Analysis

Data were expressed as the mean plus or minus SD. The significance of the data were determined by using Student *t* test for the evaluation of angiogenesis, lymphangiogenesis, plasma VASH1 concentration, and tumor-related photons, and by performing Fisher exact test

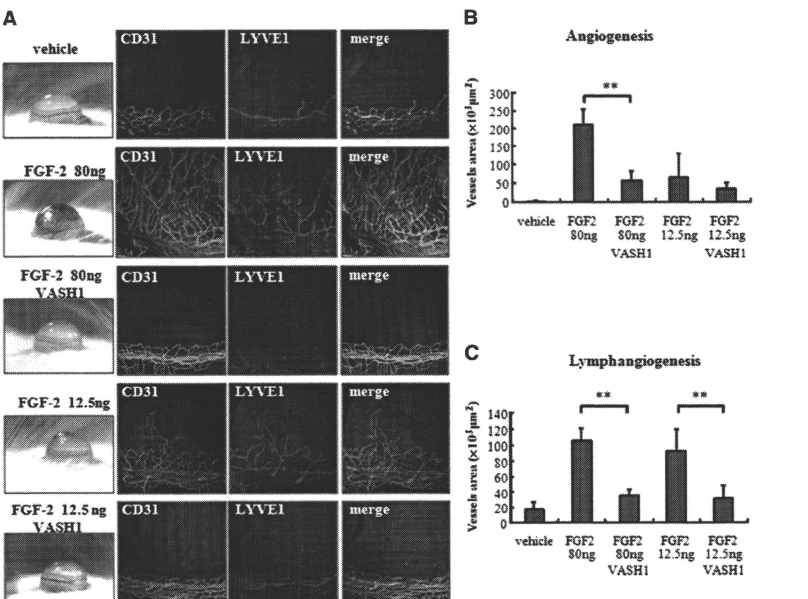

Figure 3. VASH1 inhibits angiogenesis and lymphangiogenesis induced by FGF2. **A:** Pellets containing 80 ng (high dose) or 12.5 ng (low dose) of FGF2 plus or minus 4 ng of VASH1 were inoculated into the mouse cornea. Fourteen days after the inoculation, the corneas were harvested and immunostained for LYVE1 (red) or CD31 (green). Scale bar = 200 μm. Experiments were repeated at least 3 times, and representative data are shown here. **B:** The areas of CD31-positive vessel were quantified, and the means and SDs are shown. At the higher dose, FGF2 induced angiogenesis, and VASH1 significantly inhibited the angiogenesis induced by FGF2. $n = 5$, $^{**}P < 0.01$. At the lower dose, FGF2 did not significantly induce angiogenesis. $n = 5$. **C:** The areas of LYVE1-positive vessel were quantified, and the means and SDs are shown. At both the higher and lower doses, FGF2 induced lymphangiogenesis, and VASH1 significantly inhibited the lymphangiogenesis induced by either dose of FGF2. $n = 5$, $^{**}P < 0.01$.

for the evaluation of lymph node metastasis. Statistical significance was defined as a P value less than 0.05.

Results

VASH1 Exhibits Broad-Spectrum Antiangiogenic and Antilymphangiogenic Activities

Earlier we used human VASH1 protein in various mouse models and showed its antiangiogenic activity.[13,16–18] A recent study indicated that the antiangiogenic effect of mouse VASH1 protein was not distinguishable from that of human VASH1 protein in a mouse model.[20] Here we used human VASH1 protein. VEGF-A strongly induces both angiogenesis and lymphangiogenesis in the mouse cornea.[21] By immunostaining a mouse cornea for CD31 as a marker for BECs and for LYVE1 as a marker for LECs, we confirmed this activity of VEGF-A (Figure 1A), and further showed that the co-administration of recombinant VASH1 protein with VEGF-A almost completely blocked VEGF-A–induced angiogenesis and lymphangiogenesis (Figure 1, B and C).

We next applied VEGF-C, a principal stimulator of lymphangiogenesis, to the mouse cornea. In agreement with a previous report,[5] VEGF-C induced lymphangiogenesis and also angiogenesis to some extent when administered alone to mouse corneas, and co-administration of VASH1 with VEGF-C abolished both lymphangiogenesis and angiogenesis induced by VEGF-C (Figure 2A). Quantitative analysis confirmed these effects of VASH1 (Figure 2, B and C).

We further administered growth factors other than VEGF family members that are known to have stimulatory effects on angiogenesis and lymphangiogenesis. It is reported that FGF2 induces both angiogenesis and lymphangiogenesis at a higher dose (80 ng per pellet), but primarily induces lymphangiogenesis at a lower dose (12.5 ng per pellet).[22] We confirmed these differential effects of FGF-2 and further demonstrated that co-administration of VASH1 with high-dose FGF2 almost completely blocked both angiogenesis and lymphangiogenesis (Figure 3, A–C). PDGF-BB is reported to induce intratumoral lymphangiogenesis and to promote lymphatic metastasis.[6] VASH1 inhibited both angiogenesis and lymphangiogenesis induced by PDGF-BB (Figure 4, A and B).

Taken together, these results indicate that VASH1 has broad-spectrum antiangiogenic and antilymphangiogenic activities.

VASH1 Inhibits Tumor Lymphangiogenesis and LN Metastasis

Next, we proceeded to test the effect of VASH1 in the tumor xenograft model. We injected adenovirus vector encoding the human *VASH1* gene (AdVASH1) into a tail vein of mice. Adenovirus vector encoding the *β-galactosidase* gene (AdLacZ) was used as a negative control. This vector should supply sufficient VASH1 protein to regulate angiogenesis, as described previously.[17] Indeed, Western blotting for human VASH1 revealed that human VASH1 protein accumulated in various organs 10 days after the viral injection (Figure 5A). Differences in molecular size should be attributable to the FLAG tag in recombinant VASH1 protein for control,[11] and posttranslational processing of VASH1 protein in mice.[19] ELISA analysis recognizing both murine and human VASH1 revealed that the plasma concentration of VASH1 increased about threefold (Figure 5B).

We then inoculated the flanks of SCID mice with highly LN-metastatic human non-small cell lung cancer (LNM35) cells.[23] Adenovirus vectors were injected on day 0 and day 14, and tumor tissues were collected on day 28. Tumor angiogenesis was analyzed by immunostaining VECs for CD31. Blood vessels were distributed within the tumor; and, as expected, the blood vessel area was significantly reduced in the AdVASH1-injected group (Figure 5C). Tumor lymphangiogenesis was analyzed by immunostaining for LYVE1. We simultaneously performed F4/80 immunostaining to distinguish LYVE1-expressing macrophages as described.[24] LYVE1-positive and F4/

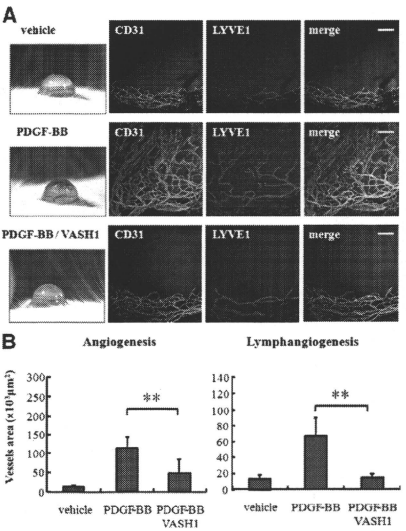

Figure 4. VASH1 inhibits angiogenesis and lymphangiogenesis induced by PDGF-BB. **A:** Pellets containing 160 ng of PDGF-BB plus or minus 4 ng of VASH1 were inoculated into the mouse cornea. Fourteen days after the inoculation, corneas were harvested and immunostained for LYVE1 or CD31. Scale bar = 200 μm. Experiments were repeated at least three times, and representative data are shown here. **B:** The area of CD31-positive vessel was quantified, and the means and SDs are shown. VASH1 significantly inhibited the angiogenesis induced by PDGF-BB. $n = 5$, $^{**}P < 0.01$. The area of LYVE1-positive vessel was quantified, with means and SDs shown. VASH1 significantly inhibited the lymphangiogenesis induced by PDGF-BB. $n = 5$, $^{**}P < 0.01$.

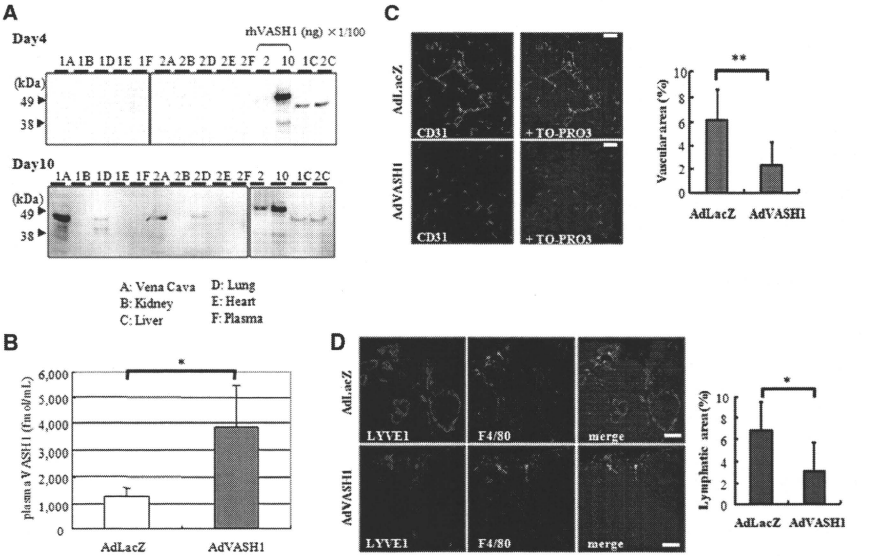

Figure 5. Adenovirus-mediated systemic delivery of VASH1 protein inhibits tumor lymphangiogenesis of LNM35 cells. **A:** AdVASH1 or AdLacZ (1×10^9 pfu) was injected into a tail vein of mice. Various organs were collected from two mice on day 4 and day 10 after the injection, and Western blotting for human VASH1 protein was performed as described in *Materials and Methods*. Recombinant human VASH1 protein with a triple repeat of the FLAG tag (rhVASH1) was used as a control. **B:** Plasma samples were collected 10 days after the injection, and the concentration of VASH1 was determined by ELISA. $n = 5$, $^*P < 0.05$. **C:** LNM35 cells were inoculated subcutaneously, and adenovirus vectors were injected into the tail vein of mice on day 0 and day 14. On day 28, the mice were sacrificed and tumors were resected. Tumor sections were immunostained for CD31 (green), and TO-PRO3 (blue) was used for nuclear staining. Scale bar = 200 μm. The intratumoral CD31-positive vascular area was quantified and expressed as % of a field. The means and SDs are shown. Tumor angiogenesis was significantly inhibited in the AdVASH1-injected mice. $n = 13$ (AdLacZ), $n = 12$ (AdVASH1), $^{**}P < 0.01$. **D:** Tumor sections were immunostained for LYVE1 (red) and F4/80 (green). TO-PRO3 (blue) was used for nuclear staining. Scale bar = 100 μm. The peritumoral LYVE1-positive and F4/80-negative vascular area was quantified and expressed as % of a field. The means and SDs are shown. Tumor lymphangiogenesis was significantly inhibited in the AdVASH1-injected mice, $n = 13$ (AdLacZ), $n = 12$ (AdVASH1), $^*P < 0.05$.

80-negative lymphatic vessels were distributed in the peri-tumoral region (Figure 5D). Quantitative analysis revealed that lymphatic vessels in the peritumoral region were significantly reduced in area in the AdVASH1-injected group (Figure 5D).

The regional axillary LNs were recovered on day 28. LN size was measured, and LN metastasis was determined by histological analysis. VASH1 significantly inhibited LN metastasis, as LN metastasis occurred in 14 of 17 AdLacZ-injected mice, but in only 4 of 16 AdVASH1-injected mice (Figure 6A). It has been described that lymphangiogenesis in the regional LNs occurs before LN metastasis and determines tumor dissemination beyond the regional LNs.[25,26] Recovered LNs were therefore immunostained for CD31 and LYVE1 to analyze angiogenesis and lymphangiogenesis (Figure 6B). Angiogenesis was not increased in either metastasis-negative or metastasis-positive LNs when compared with LNs isolated from non–tumor-bearing mice (normal LNs), but was significantly decreased in AdVASH1-injected mice when compared with the AdLacZ-injected mice (Figure 6C). In contrast, lymphangiogenesis was significantly augmented in the metastasis-negative LNs of the AdLacZ-injected mice, and was abolished in those the AdVASH1-injected mice (Figure 6C). These results suggest that VASH1 inhibited lymphangiogenesis in regional LNs before the establishment of LN metastasis.

We tested whether VASH1 impaired normal vessels in mice. Tracheal mucosa was immunostained for CD31 and LYVE1. We did not detect any morphological changes in blood or lymphatic vessels of mice injected with AdVASH1 (Figure 7A) Quantitative analysis revealed that VASH1 did not alter the area of blood or lymphatic vessels (Figure 7B).

To further show the effect of VASH1 on LN metastasis, we performed orthotopical inoculation of LN metastatic human breast cancer (231LN-Luc-1) cells. Moreover, because of the limitation of the gene therapy approach in cancers, we applied recombinant VASH1 protein. We inoculated 231LN-Luc-1 cells into the abdominal mammary fat pad of mice in the presence of recombinant VASH1 protein. We then injected recombinant VASH1 protein locally, because of the obstacle of using recombinant VASH1 protein for systemic administration. There

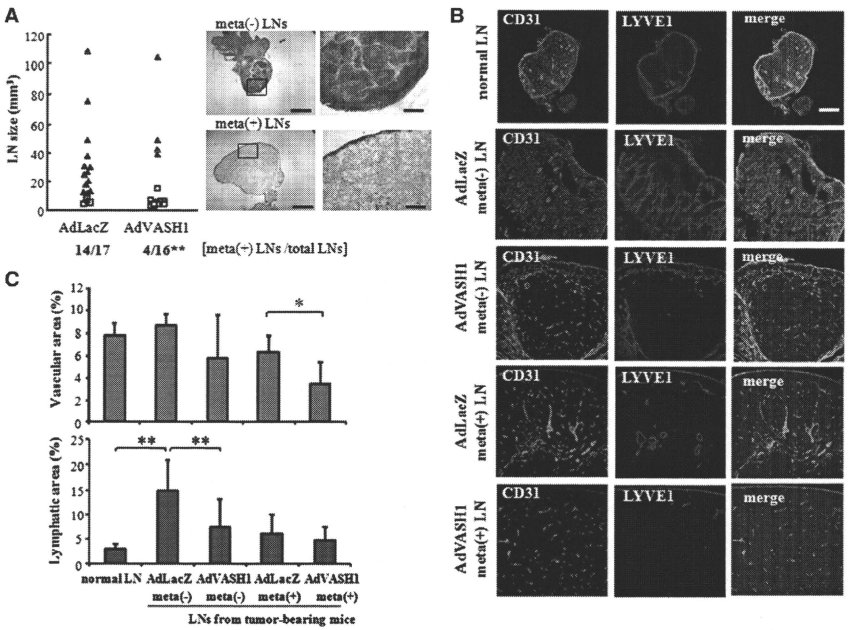

Figure 6. VASH1 inhibits LN metastasis of subcutaneously inoculated LNM35 cells. **A:** Axillary LNs were recovered. LN size was measured, and the size of LNs and the presence or absence of LN metastasis is shown. The frequency of LN metastasis in AdVASH1-injected mice was significantly lower, $^{**}P < 0.01$. Experiments were repeated three times, and representative data are shown here. LN metastasis was determined by histological analysis. Boxed fields on the left were enlarged and shown on the right. Scale bars = 500 μm on the left and 100 μm on the right. **B:** LNs were immunostained for CD31 (green) and LYVE1 (red). TO-PRO3 (blue) was used for nuclear staining. Scale bar = 200 μm. **C:** The CD31-positive and LYVE1-positive vessel areas were quantified and expressed as % of a field. The means and SDs are shown. The area of lymphatic vessels was significantly decreased in the metastasis-negative LNs of the AdVASH1-injected mice, whereas the area of blood vessels was significantly decreased in the metastasis-positive LNs of the AdVASH1-injected mice. $n = 8$ (AdLacZ meta+ and AdVASH1 meta-), $n = 4$ (normal LN, AdLacZ meta- and AdVASH1 meta+), $^{*}P < 0.05$, $^{**}P < 0.01$.

was a significant decreased in the bioluminescence in the VASH1-injected group (Figure 8).

Discussion

VASH1 was originally isolated as a VEGF-A–inducible angiogenesis inhibitor.[13] Here we assessed the effect of VASH1 on lymphangiogenesis, and explored its broad-spectrum antiangiogenic and antilymphangiogenic activities. Our findings are the first demonstration that a molecule intrinsic to the endothelium exhibits such activities.

We first applied VASH1 in combination with VEGF-A to the mouse cornea. VEGF-A induced both angiogenesis and lymphangiogenesis, and co-administration of VASH1 abolished those effects of VEGF-A. VEGF-A can induce lymphangiogenesis by affecting LECs directly or indirectly.[27,28] One means by which VEGF-A indirectly induces lymphangiogenesis is by mediating angiogenesis, which increases the local accumulation of inflammatory cells and thus the supply of lymphangiogenic factors such as VEGF-C.[29–31] Because VASH1 inhibited angiogenesis, VASH1 might exhibit its antilymphangiogenesis activity via the indirect route. To further clarify the effect of VASH1 on lymphangiogenesis, we replaced VEGF-A with VEGF-C, a principal and direct lymphangiogenesis stimulator. The result showing that VASH1 inhibited VEGF-C–stimulated lymphangiogenesis supports the direct antilymphangiogenesis activity of VASH1. Notably, VASH1 inhibited FGF2- and PDGF-BB–induced angiogenesis and lymphangiogenesis as well. Thus, the inhibitory effect of VASH1 is not restricted to the phenomena induced by the VEGF family members.

We focused our attention on the antilymphangiogenic activity of VASH1, as tumor lymphangiogenesis is recognized as a therapeutic target for the prevention of LN metastasis. We experimentally used an adenovirus vector, and showed that VASH1 delivered by this means inhibited tumor lymphangiogenesis and LN metastasis in a mouse xenograft model. The injection of

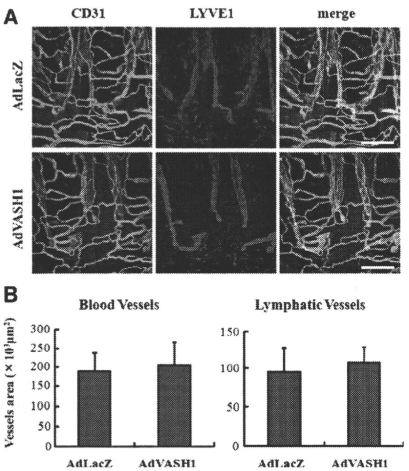

Figure 7. VASH1 does not damage normal vessels. **A:** A mouse trachea was collected on day 28, and its mucosa was immunostained for CD31 (green) and LYVE1 (red). Scale bar = 200 μm. No morphological changes were evident in the AdVASH1-injected mice. **B:** The areas of blood vessels and lymphatic vessels were quantified, and the means and SDs are shown. $n = 5$. No changes in blood or lymphatic vascular areas were evident.

AdVASH1 via a tail vein caused the synthesis of VASH1 protein in the liver. The accumulation of human VASH1 protein detected in various organs indicates that this procedure allowed us to supply human VASH1 protein systemically. The high affinity of VASH1 for heparin should be the reason for this local accumulation.[19]

As expected, AdVASH1 inhibited tumor lymphangiogenesis and regional LN metastasis. We further tested lymphatic vessels in the regional LNs, and found that lymphangiogenesis was significantly augmented in the metastasis-negative LNs and was inhibited by AdVASH1. However, lymphangiogenesis was no more augmented in the metastasis-positive LNs in the AdLacZ control. We speculate that this decrease in lymphatic vessels in the metastasis-positive LNs in the AdLacZ control might be attributable to the occupation of LNs by metastatic cancer tissues (Figure 6A), as lymphatic vessels are rarely present within cancer tissues.[32]

We previously reported the antitumor effect of VASH1 to occur through inhibition of angiogenesis.[13,18] Antiangiogenic therapy is currently being used clinically to inhibit tumor angiogenesis and tumor growth by targeting VEGF-A–mediated signaling, but one of the problems with this treatment is drug resistance.[33,34] Cancer cells switch to producing other factors such as FGF2 to combat the antiangiogenic therapy when they are treated with VEGF-A targeting monotherapy.[33] PDGF-mediated signaling is another pathway that is activated in cancers.[35] Importantly, FGF2 and PDGF-BB synergistically promote tumor neovascularization and distant metastasis.[36] The fact that VASH1 exhibited broad-spectrum antiangiogenic activity, including that against FGF2 and PDGF-BB, reveals an advantageous characteristic of it.

It has been reported that the blockade of VEGFR3 signaling inhibits tumor lymphangiogenesis and LN metastasis.[37] Thus, with analogy to the antiangiogenesis therapy, VEGFR3 signaling is proposed to be an appropriate target for the inhibition of lymphangiogenesis. It is not clear yet whether resistance would occur when VEGFR3 signaling is blocked.[37] Nevertheless, because FGF2 and PDGF-BB, which are candidates to cause drug resistance in antiangiogenic therapy, promote lymphangiogenesis as well, the broad-spectrum antiangiogenic and antilymphangiogenic activities of VASH1 are noteworthy.

In summary, our present study shows that the intrinsic factor VASH1 has broad-spectrum antiangiogenic and antilymphangiogenic activities, thus affording it the potential to inhibit tumor lymphangiogenesis and LN metastasis. We propose that VASH1 should be tested further for controlling tumor angiogenesis and lymphangiogenesis.

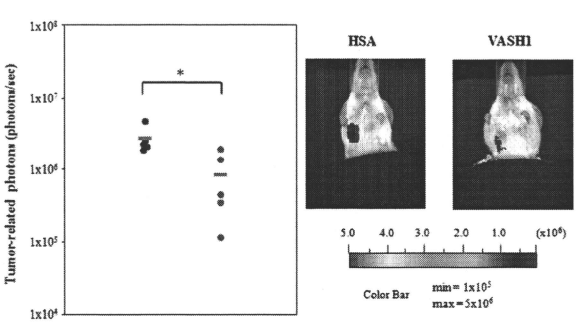

Figure 8. VASH1 inhibits LN metastasis of orthotopically inoculated 231LN-Luc-1 cells. 231LN-Luc-1 cells (5×10^6) were inoculated into the abdominal mammary fat pad of mice. Recombinant VASH1 protein or HSA was applied locally. Auxiliary LN metastasis was analyzed by the bioluminescence imaging technique. LN metastasis on day 32 was quantified as photons/sec on the left. $n = 5$, $^*P < 0.05$. Representative photos on day 32 are shown on the right. The color-bar indicates the value (photons/sec) for metastatic tumors.